Progress In Electromagnetics Research C, Vol. 66, 55–61, 2016

Wireless Power Transfer at Sub-GHz frequency for Capsule Endoscope

Keke Ding[1, 2, *], Ying Yu[1, 2], Hong Lin[1, 2], and Jingming Xie[1]

Abstract—Wireless power transfer system to capsule endoscope at sub-gigahertz (GHz) frequency is presented. Compact self-resonant antennas are designed to realize the transcutaneous power transfer. Experiment shows that at a distance of 5 cm, the designed system operating at 433.9 MHz can realize 1.21% power transfer efficiency (PTE) through duck intestine and porcine multilayered tissues, that is, 47.55 mW power delivered to load (PDL) at the specific absorption rate (SAR) occupational exposure limitation.

1. INTRODUCTION

Wireless capsule endoscopy (WCE) for diagnosing gastrointestinal (GI) tract is a great breakthrough with its noninvasive and whole-digestive-tract detection. Currently, available endoscopic capsules use two coin-shaped batteries to provide typically 25 mw power for limited 6–8 hours [1]. To get more available and more sustained energy, wireless power transfer (WPT) has been proven to be a promising technology for WCE out-body powering [2].

Inductive coupling is a well-accepted type of WPT to WCE [1]. However, large volume of power transmitter with high ac voltage limits the patient's action [3]. Magnetic resonance applied to WCE [4] has reduced the transmitter size, but the series resonant capacitors increase the power loss and reduce the power transfer efficiency (PTE). Though radiative coupling power transfer has also been researched for WCE [5], the calculation model which consists of two layers of muscle is inaccurate for modeling human body.

In this paper, a portable, effective and safe WPT system is aimed to be built for WCE. Herein, based on the biological model with multi-layered tissues, antennas at sub-gigahertz (GHz) frequency are designed for WPT to WCE. The specific absorption rate (SAR) is also calculated for the safety of the system. The validation adopts the HFSS simulation [6] and experimental measurements.

2. ANALYTICAL MODEL AND ANTENNA DESIGN

2.1. Biological Model

A swallowed capsule travels around the human body through the GI tract. An external device powers the capsule as well as receiving image data, while capsule endoscopy captures images and sends image data to the external device, as illustrated in Fig. 1(a).

The power transmitter (TX) in the external device and power receiver (RX) in the capsule, as well as the human abdomen, are modeled as shown in Fig. 1(b) and Fig. 1(c). Unlike free-space WPT, various biological tissues, with their conductivities and dielectric constants, are taken into account according to human anatomy. The layers of four cylinders from superficial to deep are, in order, skin,

Received 23 April 2016, Accepted 10 July 2016, Scheduled 16 July 2016

* Corresponding author: Keke Ding (dingkekedkk@163.com).

[1] College of Electronic Science and Engineering, Nanjing University of Posts and Telecommunications, Nanjing, Jiangsu 210023, China. [2] Jiangsu Provincial Engineering Laboratory for RF Integration and Micropackaging, Nanjing, Jiangsu 210023, China.

fat, muscle and GI tract with respective thicknesses listed in Table 1. The thicknesses of the fat layer and anterolateral muscle are based on statistical analysis [7]. Other layers are chosen from the characteristic range of normal computed tomography (CT) performance for adult. The height and diameter are set to be consistent with experimental settings. RX is not directly in contact with biological tissue but is insulated with air in the cylindrical GI cavity, as gastrointestinal lumen is required to be empty before GI endoscopy examination. The conductance and relative permittivity of tissues are calculated using four-term Cole-Cole model [8]. An average value of 1000 kg/m^3 is used to represent the mass density of these biological tissues.

Since the small intestine is the longest part of the GI tract with the highest conductance, the small intestine tissue with a dielectric constant of 65.27 and conductivity of 1.92 S/m at 433.92 MHz is assigned to GI tract for antenna design. RX is initially placed vertically in the middle of the GI cavity (d_{pos} = 10 mm), parallel with the TX. To investigate position-dependent WPT performance, different d_{pos}s are applied to RX in the GI tract for comparison.

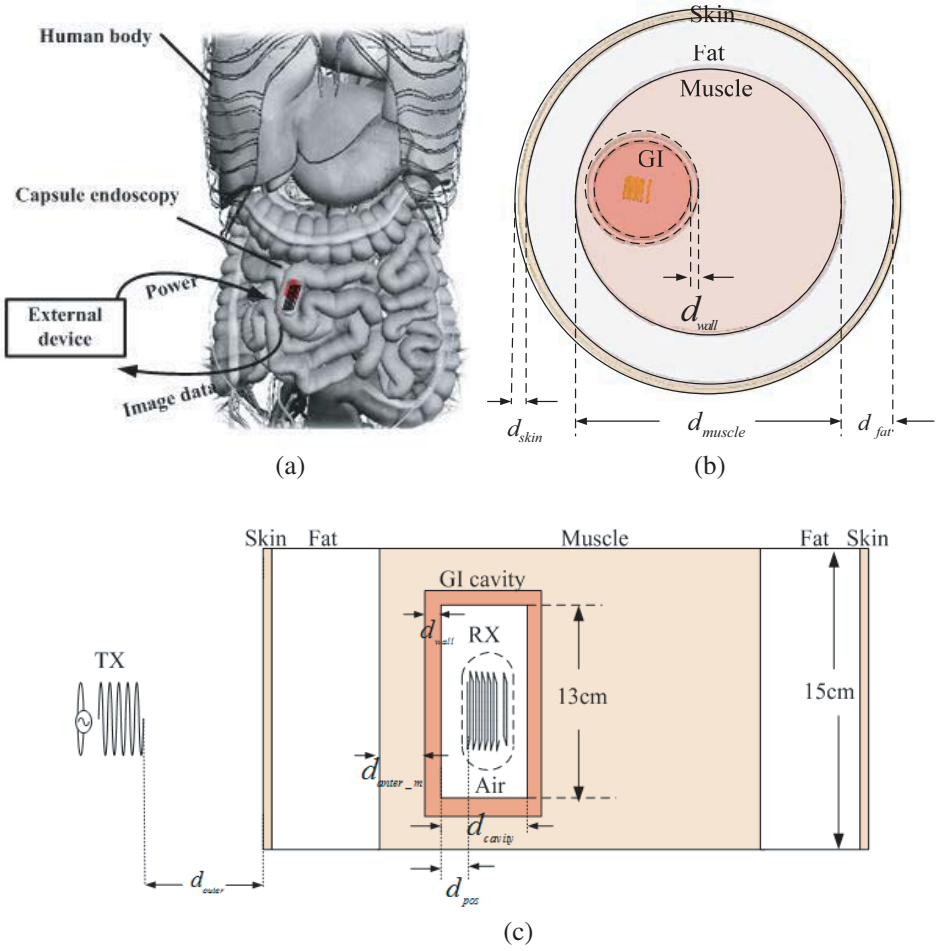

Figure 1. (a) The sketch of Capsule endoscopy (the human body adopted from Zygote Body [9]). (b) Top view of the biological model. (c) Side view of the biological model.

2.2. Antenna Design

Since study shows that sub-GHz frequency is the optimal frequency for cm-sized WPT antenna to transmit into dispersive tissue [10] and increasing the carrier frequency could reduce the antenna size, we choose 433.9 MHz as the designed power link center frequency. The frequency is within the Federal Communications Commission (FCC) industry scientific medical (ISM) band and can be compatible with

Table 1. Parameters in biological model.

Symbol	Description	Value
d_{skin}	Thickness of skin layer	2 mm
d_{fat}	Thickness of fat layer	14.83 mm
d_{muscle}	Diameter of muscle cylinder	60 mm
d_{anter_m}	Thickness of anterolateral muscle layer	3.17 mm
d_{wall}	Thickness of GI wall	2 mm
d_{cavity}	Diameter of GI cavity	29 mm
d_{outer}	Distance between the skin and the TX	20 mm
d_{pos}	Distance between the RX and the GI cavity inner side	3 mm to 17 mm

the typical video transmission frequency on the market, so that the RX might be reused as the antenna for wireless data transfer through time division multiplexing.

Similar to resonance-based WPT systems, a four-coil structure [11] is adopted. The TX antenna consists of a source coil and a sending coil, whereas the RX comprises a receiving coil and a load coil, as shown in Fig. 2. A typical self-resonant helical antenna is chosen as the sending coil, and a circular ring is used as the source coil. On the other hand, a helical antenna with rectangular cross section is designed as the receiving coil, and a rectangular ring is selected as the load coil. Since the conductor resistance decreases with the increase of wire diameter, the diameter of the copper wire here is set to 0.8 mm, for low conductor loss and easy fabrication.

Both the TX and RX are tuned to resonate at the same frequency of 433.9 MHz. It is worth to note that the RX size is confined by the capsule size of 11 mm by 22 mm typically. TX parameters are optimized to maximize the PTE. The positions and sizes of the source coil and load coil are adjusted for port impedance. To verify the feasibility, human phantom with a dielectric constant of 56.7 and conductivity of 0.94 S/m at 450 MHz [12] is used in the initial design. Then the antennas are adjusted to the parameters in the biological model above. The dimensions of the designed antennas are summarized in Table 2.

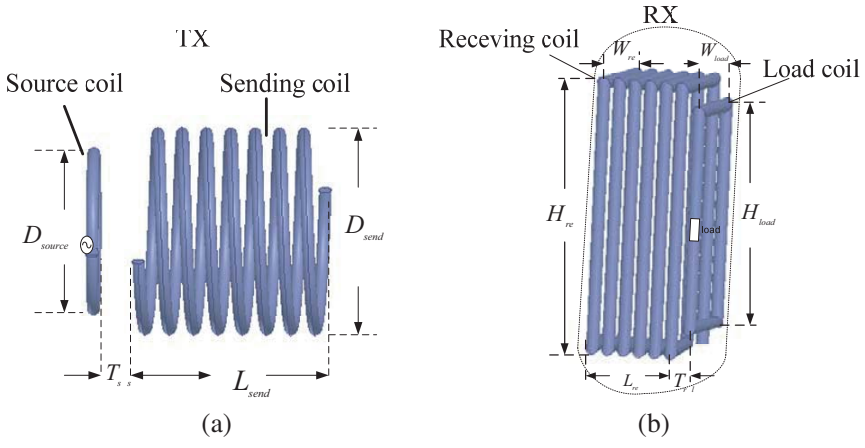

Figure 2. (a) Schematic diagram of the TX. (b) Schematic diagram of the RX.

3. INFLUENTIAL ANALYSIS ON CAPSULE MOVEMENT

Since streamline top of the capsule suffers lower resistance and objects move along the direction of small resistance [13], the RX in capsule is moving along the direction of the intestine mostly via natural peristalsis, as in the design.

Table 2. Dimensions of the TX and RX.

Symbol	Description	Value	Symbol	Description	Value
D_{source}	Diameter of the source coil	10 mm	W_{load}	Width of the load coil	5 mm
D_{send}	Diameter of the sending coil	12.50 mm	H_{re}	Height of the receiving coil	14.95 mm
L_{send}	Length of the sending coil	11.71 mm	W_{re}	Width of the receiving coil	7 mm
N_{send}	Turns of the sending coil	7.50	L_{re}	length of the receiving coil	6 mm
$T_{s\text{-}s}$	Interval between the source and sending coil	3 mm	N_{re}	Turns of the receiving coil	6
H_{load}	Height of the load coil	12.95 mm	$T_{r\text{-}l}$	Interval between the receiving and load coil	2 mm

Consider that the PTE is maximum when the TX and RX are coaxial, as described in Fig. 1(c). Magnet system [14, 15] could be applied to control the orientation of the capsule. That is, with magnet system generating and exerting a force on one side of the endoscope capsule, the cross section of RX could be maintained towards the lateral abdomen. Meanwhile, the altitude and orientation of small size TX outside could be adjusted flexibly by real-time localization system [16]. So the TX and RX could be controlled to face with each other.

Therefore, the separating distance d_{pos} is the most essential parameter for determining the actual power transfer efficiency. Fig. 3 plots the influence of the RX position on PTE. PTE is estimated by the simulated S-parameter, with impedance matched ($|S_{11}| \approx 0$).

$$PTE = \frac{|S_{21}|^2}{1 - |S_{11}|^2} \approx |S_{21}|^2 \tag{1}$$

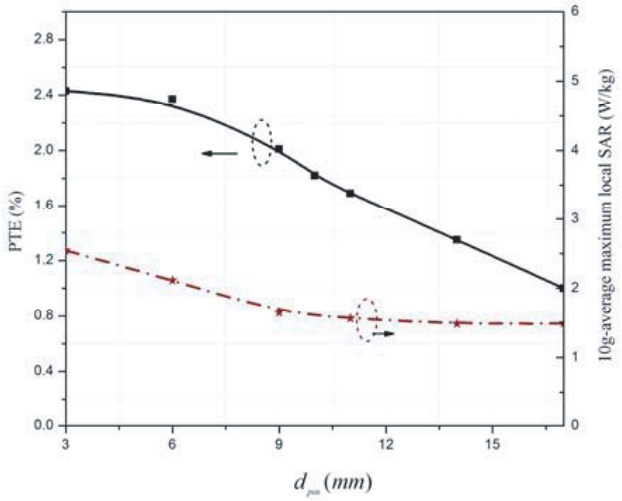

Figure 3. The influence of the RX position to PTE and SAR.

It is unavoidable that the PTE reduces with the increase of distance. However, the minimum PTE is still above 1%. Moreover, the existence of the magnet system would induce the capsule to move toward the TX side (the value d_{pos} would be small), keeping PTE in the higher range.

4. SAR CALCULATION

For biomedical applications of electromagnetic (EM) field-generating devices, the EM field absorption in the body has to be satisfied. SAR is used as a key index in international standards. The International Commission on Non-Ionizing Radiation Protection (ICNIRP) safety guideline requires 2 W/kg for public exposure and 10 W/kg for occupational exposure to be satisfied in the frequency range from 10 MHz to 10 GHz [17].

10 g-averaged maximum local SAR normalized to a 1 W input power is simulated by the fields calculator in HFSS and plotted in Fig. 3. The simulations show that the SAR is less than 2.54 W/kg and decreases with the increase of d_{pos}. Applying the occupational exposure limitation, it turns out that about at least 3.93 W power could be transmitted under the occupational exposure limitation.

5. EXPERIMENTS AND DISCUSSION

The experimental setup is shown in Fig. 4. Duck intestine and porcine abdominal tissues are used to imitate the capsule working condition. An intestine wrapped polyethylene container is covered with porcine abdominal tissues, with an incision for RX insertion. The inserted RX is placed at a distance of 3 cm from the front surface of the skin, and TX is located 2 cm from the skin. The TX and RX are fabricated initially as shown in Table 2, and the parameters are slightly tuned for the designed resonant frequency and port impedance. Table 3 lists the actual sizes of the TX and RX. L-type impedance matching networks are used for measurement. System performance is analyzed in the S-parameter measurement with vector network analyzer.

Figure 5 plots the measured and simulated S parameters. The measured S_{21} has a smaller maximum value and broader band than the simulated result. It may be caused by the following reasons. The relative permittivity and conductivity of the animal tissues are different from human tissues. The fabricated antennas have a much lower quality factor than the simulated. Impedance matching networks in the measurement bring extra loss and further reduce the system quality factor. It is measured that the maximum S_{21} is -19.17 dB at 433.9 MHz. The corresponding PTE is 1.21%.

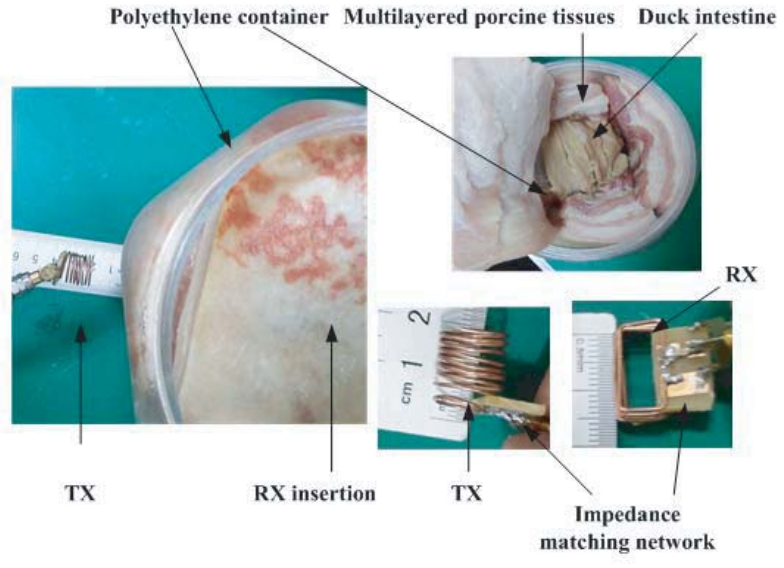

Figure 4. Experimental setup.

Table 3 compares our work with previous researches. From the comparison, it is easy to find that our small size TX replaces the traditional huge coils, so that it can be carried with convenience. Though little advantage on the PTE of our system, 47.55 mW power could be delivered to load with SAR occupational limitation, exceeding the existing battery.

Table 3. Performance comparison.

Study	RX size (mm) φ Diameter /(height, width), length	TX Type	TX (cm) diameter, length	Frequency (MHz)	TX-RX Distance (cm)	PTE
[4]	φ9,N/A[a]	Coils in front	8, N/A	16.47	7	0.70%
[5]	φ10, 27	Dipole array outside	N/A, 4	433.92	6.5	2.40% (simulated)
[18]	φ11.5, 11.5	Coils around	40, N/A	0.22	20	5.05%
Our work	(15.9, 7.7), 9.5[b]	Coils in front	1.33, 1.68[b]	433.9	5	1.21%

[a] N/A means "not available". [b] Our sizes in the table are the actual sizes including the intervals and the width of wires in the measurement.

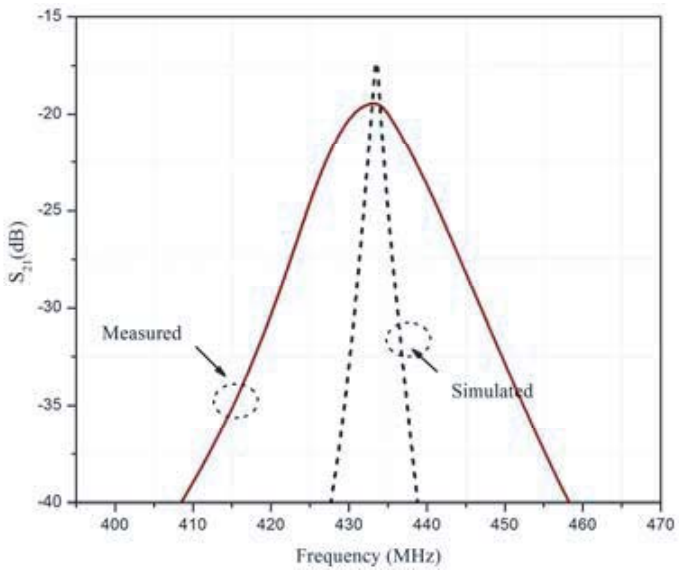

Figure 5. Measured and simulated frequency response.

6. CONCLUSIONS

We have presented the wireless power transfer system to capsule endoscopy at sub-GHz frequency. The designed TX antenna is more compact in size, which increases the portability of the system. Simulation and experiments show that 1.21% power efficiency could be achieved at a distance of 5 cm, 47.55 mw power delivered to load under SAR occupational limitation, which could fulfill the basic power requirement.

The future research efforts will focus on the optimization on the structure of RX and TX antennas to further increase PTE and reduce SAR.

ACKNOWLEDGMENT

This work was supported by the research innovation program for college graduates of Jiangsu Province (CXZZ12_0460), the open research fund of State Key Lab. of Millimeter Wave (K201412), National Natural Science Foundation of China (61302155) and Jiangsu Province Industrial Support Project of China (BE2013130).

REFERENCES

1. Basar, M. R., M. Y. Ahmad, J. Cho, and F. Ibrahim, "Application of wireless power transmission systems in wireless capsule endoscopy: An overview," *Sensors*, Vol. 14, No. 6, 10929–10951, Jun. 2014.
2. Singeap, A., C. Stanciu, and A. Trifan, "Capsule endoscopy: The road ahead," *World Journal of Gastroenterology*, Vol. 22, No. 1, 369–378, Jan. 2016.
3. Rao, S. and J. C. Chiao, "Body electric: Wireless power transfer for implant applications," *IEEE Microwave Magazine*, Vol. 16, No. 2, 54–64, Mar. 2015.
4. Na, K., H. Jang, H. Ma, and F. Bien, "Tracking optimal efficiency of magnetic resonance wireless power transfer system for biomedical capsule endoscopy," *IEEE Transactions on Microwave Theory and Techniques*, Vol. 63, No. 1, 295–303, Jan. 2015.
5. Kumagai, T., K. Saito, M. Takahashi, and K. Ito, "Design of receiving antenna for microwave power transmission to capsular endoscope," *Proc. 2011 IMWS-IWPT*, 145–148, 2011.
6. Kumagai, T., K. Saito, M. Takahashi, and K. Ito, "An introduction to HFSS: Fundamental principles, concepts and use," *Ansoft LCC*, Pittsburgh, PA, 2009.
7. Dong, D. H., W. Y. Liu, H. B. Feng, Y. L. Fu, and S. Huang, "Study of individual characteristic abdominal wall thickness based on magnetic anchored surgical instruments," *Chinese Medical Journal*, Vol. 128, No. 15, 2040–2044, Aug. 2015.
8. Gabriel, S., R. W. Lau, and C. Gabriel, "The dielectric properties of biological tissues: III. Parametric models for the dielectric spectrum of tissues," *Physics in Medicine and Biology*, Vol. 41, No. 11, 2271–2293, Apr. 1996.
9. Zygote body, https://zygotebody.com/.
10. Poon, A. S. Y., S. O'Driscoll, and T. H. Meng, "Optimal frequency for wireless power transmission into dispersive tissue," *IEEE Transactions on Antennas and Propagation*, Vol. 58, No. 5, 1739–1750, May 2010.
11. Farid, J., M. Jeetkumar, Y. Q. Yu, and Z. Z. Chen, "Design of wireless power transfer systems using magnetic resonance coupling for implantable medical devices," *Progress In Electromagnetics Research Letters*, Vol. 40, 141–151, 2013.
12. Farid, J., M. Jeetkumar, Y. Q. Yu, and Z. Z. Chen, Federal Communication Commission Office Engineering and Technology Supplement C (Ed. 01-01) to OET Bulletin 65 (ED. 97-01), Evaluating Compliance with FCC Guideline for Human Exposure to Radiofrequency Electromagnetic Fields, Additional Information for Evaluating Compliance of Mobile and Portable Devices with FCC Limits for Human Exposure to Radiofrequency Emissions, Washington, DC, Jun. 2001.
13. Shapiro, A. H., *Shape and Flow*, Heinemann Educational Publishers, Dec. 31, 1986.
14. Schmidt, S., "Method for controlling the movement of an endoscopic capsule," WO2009/127506, Oct. 22, 2009.
15. Carpi, F., N. Kastelein, M. Talcott, and C. Pappone, "Magnetically controllable gastrointestinal steering of video capsules," *IEEE Transactions on Bio-medical Engineering*, Vol. 58, No. 2, 231–234, Feb. 2011.
16. Pham, D. M. and S. M. Aziz, "A real-time localization system for an endoscopic capsule using magnetic sensors," *Sensors*, Vol. 14, No. 11, 20910–20928, 2014.
17. Pham, D. M. and S. M. Aziz, "ICNIRP guidelines for limiting exposure to time-varying electric, magnetic, and electromagnetic fields (up to 300 GHz)," *Health Physics*, Vol. 74, No. 4, 494–522, Oct. 1998.
18. Jia, Z., G. Yan, P. Jiang, Z. Wang, and H. Liu, "Efficiency optimization of wireless power transmission systems for active capsule endoscopes," *Physiological Measurement*, Vol. 32, 1561–1573, Aug. 2011.